ACS OMEGA

http://pubs.acs.org/journal/acsodf

Article

Hydrothermal Carbonization of *Searsia lancea* Trees Grown on Mine Drainage: Processing Variables and Product Composition

Ramadimetja L. Setsepu, Jibril Abdulsalam, Isabel M. Weiersbye, and Samson O. Bada*

Cite This: *ACS Omega* 2021, 6, 20292−20302

Read Online

ACCESS | Metrics & More | Article Recommendations

ABSTRACT: A 12-year-old planted woodlands *Searsia lancea* tree, grown on acid mine drainage for phytoremediation of polluted groundwater on gold and uranium mines in South Africa, was used in this research. The research describes the fuel-related characteristics and the influence of different operating conditions on the hydrothermal carbonization of the biomass and the combustion profiles of discard coal/biomass hydrochar pellets. The raw biomass was treated at temperatures ranging from 200−280 °C and residence time of 30−90 min. The hydrochar produced at 280 °C and residence time of 90 min had the highest calorific value of 29.71 MJ/kg compared to 17.23 and 16.73 MJ/kg obtained from the raw biomass and discard coal, respectively. Regression equations developed using the central composite design (CCD) indicated that the values obtained experimentally agree with the predicted values from the models for mass yield, calorific value, and ash content. The reactivity tests showed that the 100% hydrochar pellet had the highest reactivity and lowest ignition and burnout temperature compared to biocoal pellets and discard coal. The process water contained relatively low concentrations of major elements, and the study had shown that different high-grade biocoal pellets can be produced from the *S. lancea* tree.

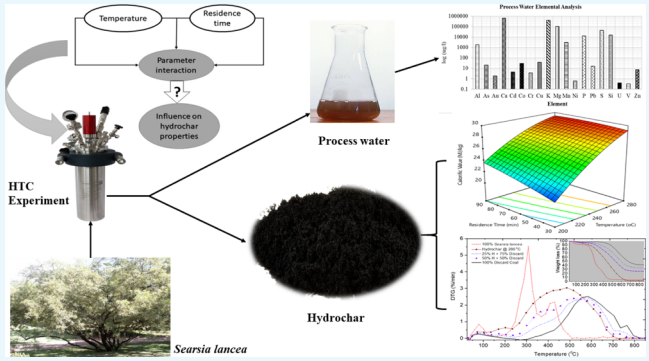

1. INTRODUCTION

The use of raw biomass for energy generation is constrained by the costs of transportation, storage and handling, and low biomass conversion ratio.[1] Raw biomass contains significant inorganic elements that can cause slagging and fouling along with a low hard-grove index (HGI), making its direct firing and milling extremely challenging without pretreatment.[2] Therefore, pretreatment, such as hydrothermal carbonization (HTC), is used to transform biomass into a predominantly carbonaceous solid hydrochar with improved physicochemical properties.[3,4]

The terms biochar,[5] biocoal,[6] and hydrochar[1,7] have all been used to describe products of the HTC process which has the advantage of directly hydrotreating wet or green biomass materials without the need for drying.[8,9] This technique has also been used for producing biofuel and upgrading solid fuels[10] as well as a precursor for soil remediation, activated carbons, catalysts, and many other carbonaceous materials.[4] HTC has also seen applications in upgrading other biomass types such as municipal solid waste,[11−14] algae,[8,15] sewage sludge,[6,15] agricultural waste,[9] and swine manure[16] to produce more desirable carbonaceous products.

There is an extensive body of the literature regarding the influence of operational factors on the hydrothermal treatment of biomass, sewage sludge, and wastewater solids.[6,17] A significant processing factor is the reaction temperature.[17] For example, in the co-hydrothermal carbonization (Co-HTC) of two different feedstocks (biomass and coal), temperature was found to be the most significant factor influencing the upgrade of coal and *Miscanthus* sp. grass biomass, and their co-blended slurries.[10] At 260 °C, the calorific value of raw *Miscanthus* sp. biomass was upgraded from 19.5 to 28.7 MJ/kg, while the energy content of the co-HTC blends increased from 24.6 to 27.9 MJ/kg. Another study of HTC operating conditions on the palletization and combustion properties of hydrochar demonstrated that temperature and residence time contributed to an increase in the energy content of raw biomass from 16.35 to 26.31 MJ/kg.[18] The hydrothermal carbonization of Tahoe Mix woody biomass utilized by Hoekman et al.[19] also displayed a massive improvement in the hydrochar's physicochemical properties. At 275 °C, the calorific vale of the woody biomass was upgraded from 20.32 to 29.67 MJ/kg, while the carbon content increased from 49.02 to 70.99%.[19] A recent study conducted by Lu et al.[20] on

Received: April 24, 2021
Accepted: June 28, 2021
Published: July 28, 2021

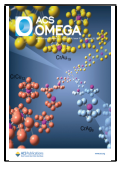

Table 1. Physicochemical Results of the *Searsia lancea* Blends, Coal Discard, and Hydrochars[a]

samples	C (%)	H (%)	N (%)	S (%)	O* (%)	TM (%)	VM (%)	FC (%)	ash content (%)	CV (%)	mass yield (%)
coal discard	48.9	2.7	1.2	1.3	1.9	2.1	20.2	35.8	42.0	16.7	
raw biomass (S11 + 12)	45.1	6.4	0.4	<0.1	35.8	8.3	69.4	18.4	3.9	17.2	
										responses	
$HC_{200, 30}$						0.7	72.4	25.5	1.4	20.3	67.3
$HC_{200, 60}$						1.9	71.1	25.9	1.1	23.1	61.9
$HC_{200, 90}$						1.3	67.4	29.1	2.3	23.5	61.8
$HC_{240, 30}$						1.8	56.9	40.1	1.3	27.6	49.5
$HC_{240, 60}$						1.8	53.8	42.8	1.6	27.9	40.1
$HC_{240, 60}$						1.8	53.8	42.8	1.6	27.9	47.1
$HC_{240, 60}$						1.8	53.8	43	1.4	26.0	46.1
$HC_{240, 90}$						1.9	50.8	44.9	2.4	27.9	75.1
$HC_{280, 30}$						2.1	46.1	50.3	1.5	29.0	59.9
$HC_{280, 60}$						0.7	48.3	49.7	1.3	29.4	59.4
$HC_{280, 90}$						2.0	46.7	50.2	1.1	29.7	71.8

[a]O*: Oxygen by difference [100 − (M + Ash + S + H + C + N)]. $HC_{T,t}$ where HC denotes hydrochar; *T*: temperature; *t*: residence time. TM: total moisture; VM: volatile matter; FC: fixed carbon; CV: calorific value; raw biomass: *Searsia lancea* (S11 + S12); wood, leaves, twigs, stump, and dried biomass.

furniture residues at a much lower temperature of 180 °C led to an increase in the biomass total carbon from 47.6 to 52.10%.

We investigated the use of biomass from the southern African indigenous semi-hardwood tree *Searsia lancea* (L.f.) F.A.Barkley (Anacardiaceae, mango family) to produce pelletized solid fuels. The tree is a dominant species of acid mine drainage (AMD)-polluted soils in the Witwatersrand basin of South Africa.[21] It is one of the species that is planted in phytoremediation woodlands for control of groundwater pollution from gold and uranium mine tailings dams in southern Africa[22,23] due to its ability to maintain transpiration rates in saline seepage and acid mine drainage.[24] These traits in turn result in the hydraulic control of polluted groundwater[25,26] and the conversion of AMD to biomass.[27] The woodlands are part of a mine closure strategy to control AMD from tailings storage facilities (TSF), and harvesting is only envisaged for the faster-growing trees. However, there is concern that these trees could be cut and used as firewood by the community,[28] rather than being used in environmentally responsible applications. The burning of biomass as firewood contributes to greenhouse gas (GHG) emissions, poor air quality, and undermines the potential of biomass grown on AMD as a clean energy source. However, a recent study by Ndou et al.[29] had shown that *Tamarix usneoides*, which is also a native species planted on the TSF has the potential of reducing SO_2 and NO_X emissions when co-fired with discard coal.

Little research has been published on the use of HTC for upgrading mixed feedstock, and little, if any, consideration has been given to biomass HTC, particularly harvested at AMD remediation sites, and cofired with high ash discard coal. This study quantified the significance of temperature and residence time (process conditions), and their interaction, on the desirable features of hydrochars produced from the *S. lancea* biomass, that is, hydrochar mass yield (%), calorific value (MJ/kg), and ash content (%). In addition, developed regression models using a response surface methodology (RSM) approach in predicting the energy characteristics of the solid fuels produced. Although RSM is a popular process optimization tool, it has not been used in predicting the physiochemical properties of hydrothermally pelletized *S. lancea*.

2. RESULTS AND DISCUSSION

2.1. Physicochemical Characterization. The proximate analysis results from the blend of two *S. lancea* trees (S11 and S12) harvested from the Mispah sites, along with the discard coal and the hydrochars are shown in Table 1. The discard coal reported a higher sulfur content of 1.34% compared to the raw biomass and the highest ash content of 41.95% of all samples tested. The energy yield derived from the *S. lancea* hydrochars is also included on the table. The volatile matter content was seen to decrease with the severity of HTC conditions, while fixed carbon increased with an increasing process temperature, and the trend was found to be similar to results available in the literature.[1,3,36] For the 200 °C isotherm, the energy yield increases from 79.09 to 84.12% with an increasing residence time of 30 and 90 min, respectively. At the highest temperature of 280 °C, the energy yield increases from 59.86 to 71.82% from 30 to 90 min, respectively. However, the energy yield at 250 °C isotherm displays a decreasing trend with increasing reaction severity from 30 to 90 min. All characterization tests were performed three times to verify the repeatability and the stated average value.

The relationship between the proximate results and individual calorific values for the raw biomass and different hydrochars produced is presented in Table 1. An increase in temperature was associated with a decrease in volatile matter and an increase in the hydrochars' calorific value. For a 30 min residence time interval, the calorific value had a range of 17.23 to 20.27 MJ/kg at 200 °C, 17.23 to 27.55 MJ/kg at 240 °C, and 17.23 to 28.97 MJ/kg at 280 °C. The fixed carbon content and calorific values were more pronounced with the increase in the residence time. The changes in the energy characteristic and quality of the hydrochar produced are due to the modification to the structure of the biomass utilized at high temperatures and pressure. The decomposition of the hydroxyl group along with the hemicellulose of the *S. lancea* biomass is responsible for the increase in the fixed carbon and calorific value, with the majority of the lignin remaining in the solid hydrochar. The increase observed in the fixed carbon of this biomass is in agreement with that reported by Fakkaew et al.,[36] Kambo and Dutta,[1] and Hoekman et al.[3] A decrease was also noted in the moisture content of the hydrochars, as well as in the ash content of the products. The decrease noted in the ash

https://doi.org/10.1021/acsomega.1c02173
ACS Omega 2021, 6, 20292−20302

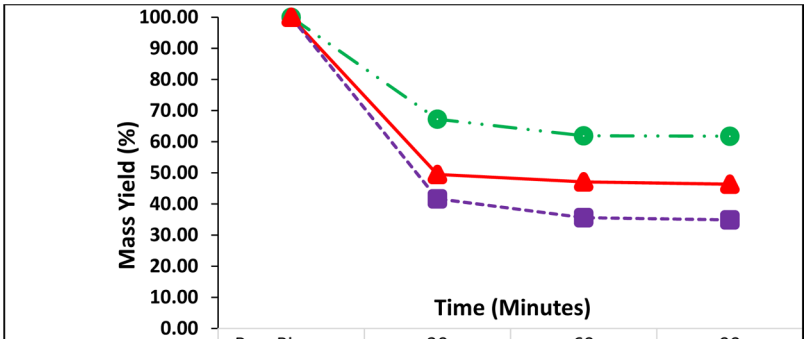

	Raw Biomass	30	60	90
Mass Yield 200 deg	100.00	67.25	61.91	61.78
Mass Yield 240 deg	100.00	49.49	47.11	46.36
Mass Yield 280 deg	100.00	41.66	35.61	34.89

Figure 1. Mass yield (%) of hydrothermal hydrochars with increase in temperature and residence time.

content of the hydrochars could be a result of the decomposition of the inorganic carbonates and oxides of minerals within the biomass into the process water liquid phase. This is expected, as Kambo and Dutta[1] reported that the HTC process resulted in an acid solvation mechanism, which is a mechanism responsible for the solubilization and leaching out of inorganic elements in the biomass; thereby leading to the reduction in the overall ash content of the solid product, which is not possible in the case of dry thermal pretreatment processes.[1]

2.2. Influence of Temperature and Residence Time on Mass Yield of Hydrochars. The effect of temperature and residence time on the mass yield of hydrochars produced from raw *S. lancea* biomass is depicted in Figure 1. A loss in sample weight is evident with an increase in temperature and is observed to be relatively fast within the first 30 min at all temperatures. At 200 °C, the lowest degradation and depolymerization of the hemicellulose content of the sample was observed, with a mass yield of 67.25%. Increasing the temperature to 280 °C led to a further decrease in the mass yield to 41.66%, with more hemicellulose being converted into chemical energy in the form of gases and high carbon solid residues. A strong positive correlation between weight loss and temperature was observed, following a similar pattern to other studies on thermal treatment of biomass.[10,31,37] The observed decrease in mass yield can be attributed to decarboxylation and dehydration reactions, which results in the degradation of the biomass functional groups.[5,10] Reza et al.[5] reported that the biomass functional groups are converted to organic acids, thereby lowering the pH of the reaction substrates and leading to further breakdown of these structures to form a carbon-dense and high-energy material.

2.3. Data Analysis. *2.3.1. Regression Model Development.* The central composite design (CCD) was used to develop the polynomial regression equations, which describe the interactions between the process variables (temperature and residence time). The regression analysis was performed to fit the response functions of mass yield (%), ash content (%), and calorific value (MJ/kg). In addition, the regression models provide a mathematical framework for future analysis of the three responses. The empirical models achieved in terms of the process variables for the hydrochar characteristics, mass yield, calorific value, and ash content are as follows

$$\text{mass yield (\%)} = 204.75 - 0.72T - 1.04t + 2.24 \times 10^{-3}Tt + 5.35 \times 10^{-4}T^2 + 4.01 \times 10^{-3}t^2 \quad (1)$$

$$\text{calorific value}\left(\frac{\text{MJ}}{\text{kg}}\right) = (-)36.05 + 0.38T + 0.19t - 5.54 \times 10^{-4}Tt - 5.45 \times 10^{-4}T^2 - 2.21 \times 10^{-4}t^2 \quad (2)$$

$$\text{ash(\%)} = 32.96 - 0.24T - 0.91t + 6.35 \times 10^{-3}Tt + 4.61 \times 10^{-4}T^2 + 2.96 \times 10^{-3}t^2 - 1.12 \times 10^{-5}T^2t - 1.05 \times 10^{-5}Tt \quad (3)$$

where T is temperature and t is residence time, and a positive symbol in front of the constant and/or the process factors indicates a synergistic relationship with the responses, whereas a negative sign shows an opposing influence on the responses.[38] Figure 2a–c shows the predicted values compared to the measured experimental values. There is a strong relationship between the modeled and the experimental values (R^2 values of 0.9537, 0.9525, and 0.9789 for mass yield, calorific value, and ash content respectively), indicating that the regression models are adequate.

Figure 3a–c depicts the 3D surface response plots describing the combined effect of temperature and residence time on the mass yield, calorific value, and ash content of the hydrochars produced, respectively. The response surface plots were used to illustrate the effect of changing reaction temperature and residence time on the responses, while the 3D plot was used for checking the model accuracy.[39] As the figures reveal, the curve tends to fit well with the design points, which are the actual observed points. None of the design points are seen to be far above or below the surface curve, supporting the model's accuracy. The singular model term (T) had the greatest effect on mass yield, while the calorific value was influenced by both (T) and (t). The interaction model term (Tt) and time (t) had an influence on the ash content.

The analysis of variance (ANOVA) was performed to demonstrate the suitability of the model developed for each response. The ANOVA for the quadratic models of mass yield, calorific value, and ash content is shown in Tables 2, 3, and 4. The values of "Prob > F" below 0.05 indicate that the model

https://doi.org/10.1021/acsomega.1c02173
ACS Omega 2021, 6, 20292−20302

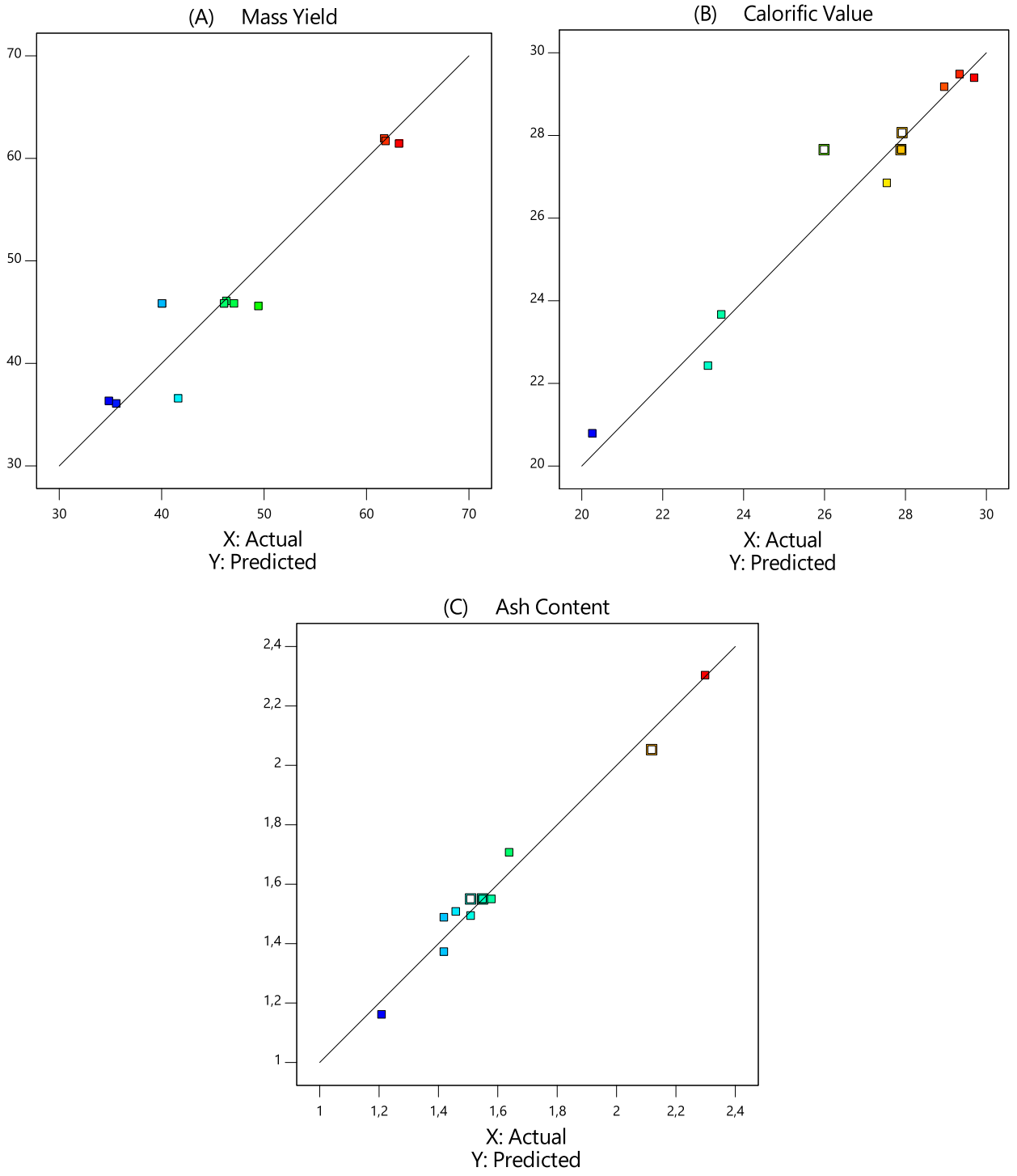

Figure 2. Predicted *vs* actual plot of (A) mass yield, (B) calorific value, and (C) ash content.

terms are significant.[34] In the case of mass yield, as can be seen in Table 2, T, which is the linear term, is the only significant model term. For the calorific value (Table 3), T and t are the significant model terms, while t, Tt, T^2, t^2, T^2t, and Tt^2 are all significant model terms for the ash content as seen in Table 4. Also assessed is the suitability of the model equations with correlation coefficients (R^2), which are 0.95 for the mass yield model equation, 0.95 for the calorific value, and 0.98 for the ash content model equation. The R^2 values for mass yield, calorific value, and ash content all exceed 0.95, which indicate agreement between experimental data and the model prediction.

2.4. Combustion Profiles of Raw *S. lancea*, Discard Coal, and Hydrochars. The thermographs presented in Figure 4 illustrate the profiles for the raw *S. lancea* biomass, discard coal, and hydrochars produced at 200, 240, and 280 °C with a residence time of 90 min. The DTG and TG plots show that the raw *S. lancea* biomass has the lowest ignition temperature compared to other fuels. The same sample also reaches its peak temperature at 308.11 °C compared to hydrochar produced at 200 °C with a peak temperature of

https://doi.org/10.1021/acsomega.1c02173
ACS Omega 2021, 6, 20292−20302

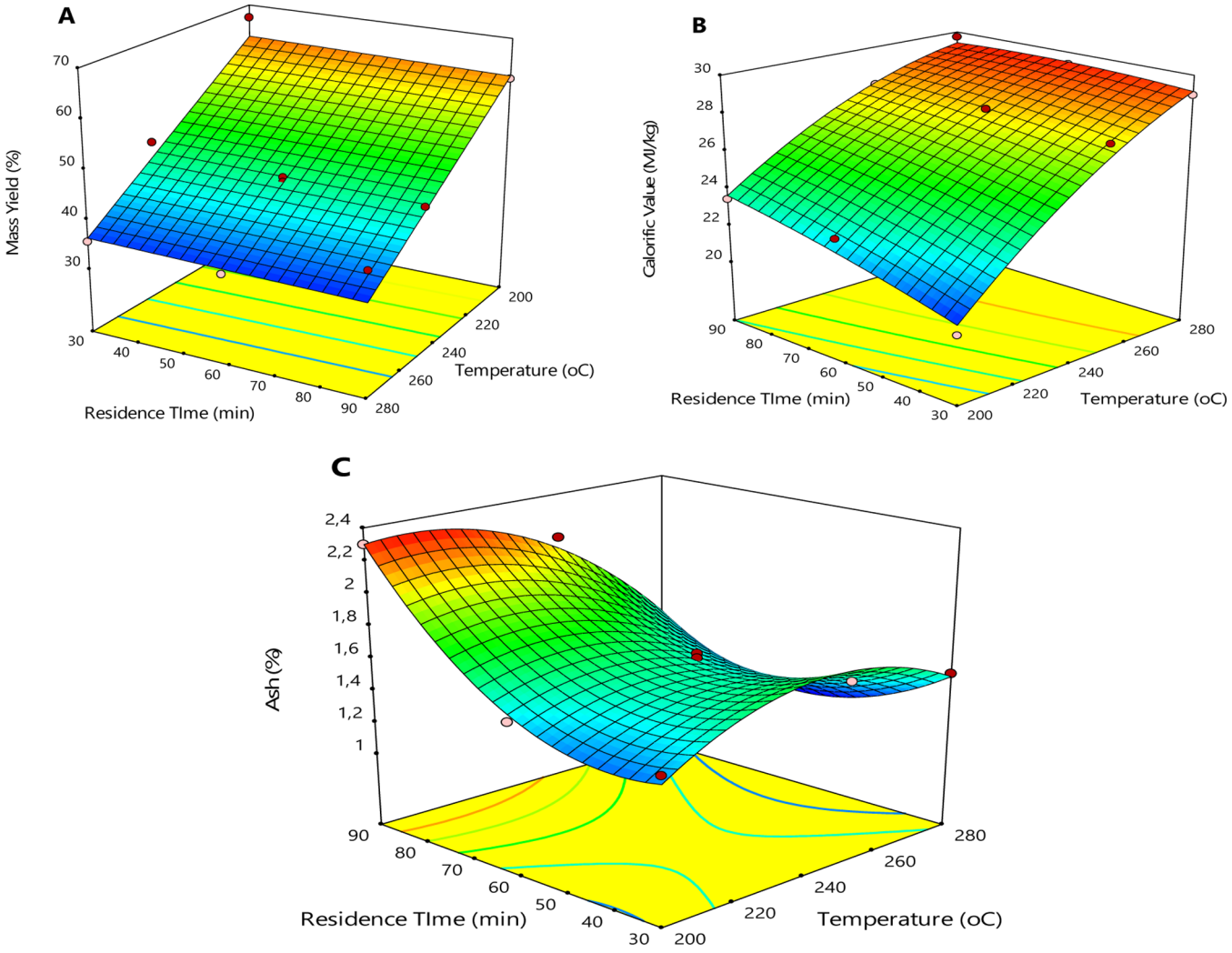

Figure 3. Combined effect of temperature and residence time on fuel characteristics of the produced hydrochars: (A) mass yield, (B) calorific value, and (C) ash content.

Table 2. ANOVA for the Response Surface Quadratic Model of Mass Yield[a]

source	sum of squares	df	mean square	*F* value	prob. >*F*	R^2
model	1197.11	5	239.42	28.82	0.0002	0.95
T	1034.38	1	1034.38	124.50	<0.0001	
t	2.50	1	2.50	0.30	0.60	
Tt	29.36	1	29.36	3.53	0.10	
T^2	1.73	1	1.73	0.21	0.66	
t^2	35.98	1	35.98	4.33	0.076	
residual	58.16	7	8.31			
lack of fit	8.63	3	2.88	0.23	0.87	
pure error	49.52	4	12.38			
cor total	1255.27	12				

[a]Df—degree of freedom; prob—probability; *T*: temperature; *t*: time.

Table 3. ANOVA for the Response Surface Quadratic Model of Calorific Value[a]

source	sum of squares	df	mean square	*F* value	prob. >*F*	R^2
model	89.88	5	17.98	28.08	0.0002	0.95
T	74.69	1	74.69	116.69	<0.0001	
t	3.56	1	3.56	5.55	0.051	
Tt	1.80	1	1.80	2.82	0.14	
T^2	1.79	1	1.79	2.80	0.13	
t^2	0.11	1	0.11	0.17	0.69	
residual	4.48	7	0.64			
lack of fit	1.55	3	0.52	0.71	0.60	
pure error	2.93	4	0.73			
cor total	94.36	12				

[a]Df—degree of freedom; Prob—probability; *T*: temperature; *t*: time.

310.50 °C, but with a higher reactivity. The higher reactivity noted for the hydrochar produced at 200 °C after the initiation of the fixed carbon (IT_{FC}) might be a result of the increase in its fixed carbon from 18.41 to 29.07%. Both samples were seen with two distinguishable peaks, showing the hemicellulose and lignin functional groups within the biomass. The hydrochar produced at a temperature of 240 °C was also seen with two peaks, but with much lower hemicellulose, while the hydrochar produced at 280 °C was seen with a single peak, which indicates a complete degradation in its hemicellulose content and increased lignin content. The hydrochar produced at 280 °C was seen with the highest burnout temperature of all the biomass samples and possesses the largest area covered under the peak because of its increase in carbon content. The area

https://doi.org/10.1021/acsomega.1c02173
ACS Omega 2021, 6, 20292−20302

Table 4. ANOVA for the Response Surface Quadratic Model of Ash Content[a]

source	sum of squares	df	mean square	*F* value	prob. >*F*	R^2
model	1.79	7	0.26	33.20	0.0007	0.98
T	0.02	1	0.02	3.09	0.14	
t	0.74	1	0.74	95.61	0.0002	
Tt	0.40	1	0.40	52.36	0.0008	
T^2	0.26	1	0.26	33.97	0.0021	
t^2	0.41	1	0.41	52.81	0.0008	
T^2t	0.33	1	0.33	42.72	0.0013	
Tt^2	0.20	1	0.20	25.72	0.0039	
residual	0.04	5	0.01			
lack of fit	0.00	1	0.00	0.04	0.84	
pure error	0.04	4	0.01			
cor total	1.83	12				

[a]Df—degree of freedom; Prob—probability; *T*: temperature; *t*: time.

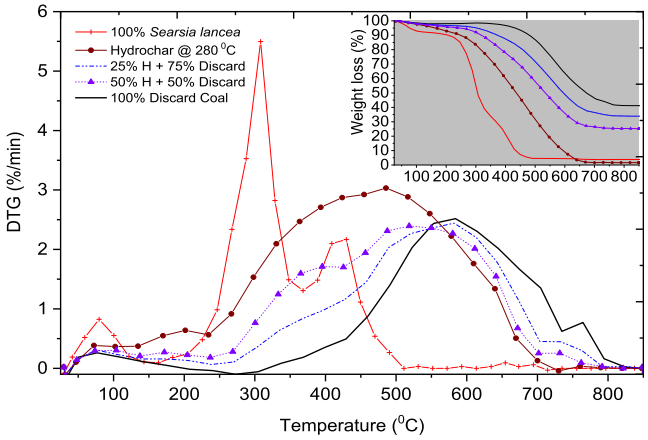

Figure 5. DTG curves for the combustion of raw *Searsia lancea* biomass, hydrochars, and hydrochar coal pellets.

covered under the peak can be denoted to be proportional to the total heat released by the fuel, which could be related to the heat content of the fuel. The discard coal was found with the highest burnout temperature of 825 °C and about 41.95% ash residue, followed by the raw *S. lancea* with about 3.91% ash residue. The reduction in the percentage ash content or noncombustibles in the hydrochar produced is due to the inorganic minerals in the biomass reporting to the liquid phase (process water).

2.5. Combustion and Cocombustion Profiles of Hydrochar and Hydrochar/Coal Pellets. The combustion profiles of the hydrochar pellet produced at 280 °C and residence time of 90 min, along with pellets produced from the blend of coal and hydrochar at different weight percentage ratios are presented in Figure 5. The dried *S. lancea* biomass has the lowest ignition temperature, followed by the hydrochar pellet produced at 280 °C and holding time of 90 min. It was observed from the DTG profile that as the percentage of coal in the blend increases, the ignition temperature of the samples moves to a higher temperature region. The 25% hydrochar + 75% discard coal pellet was seen to be more compatible with the discard coal pellet, in terms of combustion reactivity and similar burnout temperature. The burnout temperature of the discard coal used was reduced with the addition of hydrochar. The weight loss curve (TG) shows an increase in the sample's weight loss as the percentage ratio of coal in the blend decreases for all samples, and the 100% hydrochar has the lowest noncombustible residue. In summary, it can be noted that the combustion efficiency of a high ash discard coal can be improved by pelletizing it with hydrothermally pretreated biomass, and the blend with the higher discard coal mass has a close compatibility with the coal.

2.6. Analysis of Hydrothermal Process Water. *2.6.1. Organic Compounds.* The dissolved organic compounds in the process water were determined by gas chromatography linked to mass spectrometry using a Shimadzu GCMS-2010 (Table 5). Hexadecenoic acid, 2,3 bis had the highest concentration (11.87%), followed by tetradecane (9.32%); both aliphatic hydrocarbons can only be extracted with a super-heated water steam. The process water of HTC is known to contain large quantities of dissolved organic compounds, such as organic acids (formic, acetic, lactic, and propionic acid), sugars (glucose, fructose, and

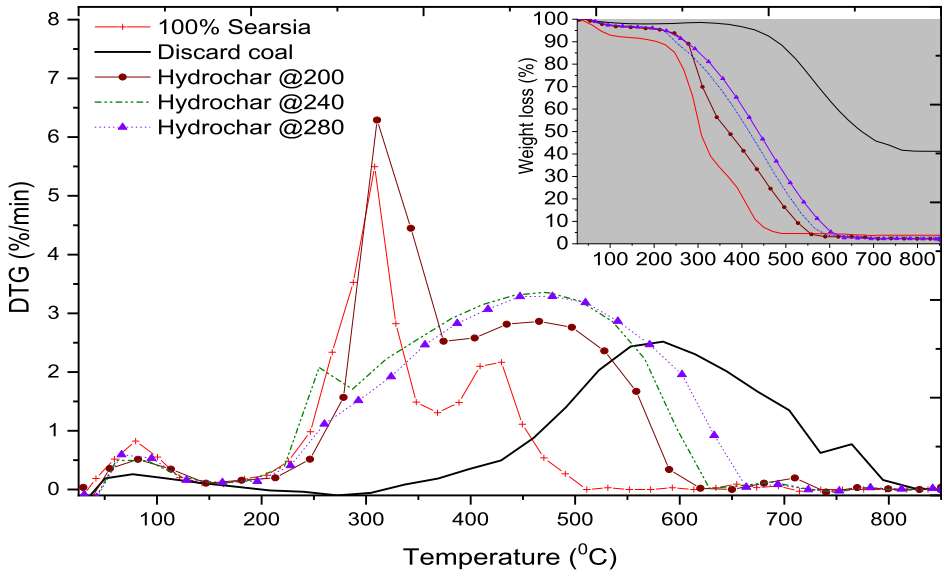

Figure 4. DTG curves for the combustion of raw *Searsia lancea* biomass, coal, and hydrochars.

https://doi.org/10.1021/acsomega.1c02173
ACS Omega 2021, 6, 20292−20302

Table 5. Organic Compounds in the Process Water

ID no.	compound	retention time (minutes)	area (%)
1	furan,2,3,5-trimethyl	4.89	1.27
2	phenol, 2,6-dimethoxy	5.33	2.93
3	3,5-methano-2*H*-cyclopenta[*b*]furan-2,4)	7.26	2.39
4	ethanone,2-azido-1-(4-methyl-3-furazanyl	7.40	5.04
5	1-hydroxylinalool	7.45	2.61
6	pentadecane	7.53	4.72
7	tetradecane	9.69	9.32
8	heptadecane	12.04	2.06
9	4-oxo-beta-isodamascol	14.23	2.85
10	2-bromotetradecane	14.53	1.82
11	1-butanethiol 3-methyl	14.94	1.84
12	3-oxo7,8-dihydro-alpha-ionol	18.42	1.80
13	pentadecanoic acid	18.83	6.34
14	1,1-dichloro-2-propylcyclopropane	18.97	2.07
15	dimethylmalonic acid, 2-isopropoxypheny	19.05	2.29
16	3-(aminomethyl)-5-*tert*-butyl-2	19.46	2.70
17	10-oxocyclodec-2-enercarboxylic acid, meth	20.27	1.97
18	1,8-diethyl-3,6-diazahomoadamantan-9-ol	20.45	1.28
19	9,12-octadecadienoic acid, (Z)	20.67	2.56
20	9,17-octadecadienal, (Z)	21.07	6.28
21	1,5-anhydro-2,6-di-*O*-di-*O*-methyl	21.58	1.41
22	bicycol[2,2,1]heptan-2-amine,*N*,*N*,1,7,7-P	22.03	1.32
23	decanoic acid	23.62	2.58
24	heptadecanoic acid, ethyl ester	24.41	1.21
25	11-bromo-1,1-dideuterioundecane	25.18	1.37
26	2*H*-pyran-2-acetic acid, tetrahydro	25.33	1.67
27	8-nonynoic acid	27.14	1.55
28	dimethyl2-methylsuccinate	27.35	1.61
29	decanedioic acid, diethyl ester	27.53	1.35
30	octadecanoic acid,2-(2-hyxyethoxy)ethyl	27.63	1.25
31	*cis*-*p*-mentha-1(7),8-dien-2-ol	27.94	1.70
32	(1alpha,3beta,4beta)-*p*-menthane-3,8-diol	28.19	4.06
33	hexadecanoic acid, 2,3-*bis*[(trimethylsilyl)]	28.71	11.87
34	germacyclopenten-3	29.04	1.47
35	hexadecane, 1,16-dichloro	29.13	1.44

xylose), furans (furfural and 5-HMF), and phenols (phenol, guaiacol, cresol, and catechol).[40] All these compounds are typical of decomposed biomass in the natural environment, but high concentrations in discharge can pollute the receiving waterbodies. Therefore, the quality of HTC water residue should be monitored and treated or diluted before discharge.

2.6.2. Dissolved Inorganic Matter in the HTC Process Water. The inorganic elements in biomass or any solid fuel can be classified as major or trace elements. Their concentration in the wastewater provides an insight into its treatment prior to discharge or usage. The most abundant elements found in the wastewater from this study were calcium (Ca) > potassium (K) > magnesium (Mg) > sulfur (S) Figure 6. Sodium (Na), Iron (Fe), titanium (Ti), and mercury (Hg) were not detectable. Mercury levels were negligible to nondetectable in the raw tree biomass, whereas Na and Fe were present at trace levels.[26] This indicates that all the Fe and Na might have been retained in the hydrochar. Contaminants of concern in the process water are copper (Cu), chromium (Cr), cobalt (Co), cadmium (Cd), arsenic (As), vanadium (V), nickel (Ni), zinc (Zn), lead (Pb), and uranium (U), all present at concentrations which approach or exceed the legal limits for discharge to fresh waterbodies (Figure 6). The gold (Au)

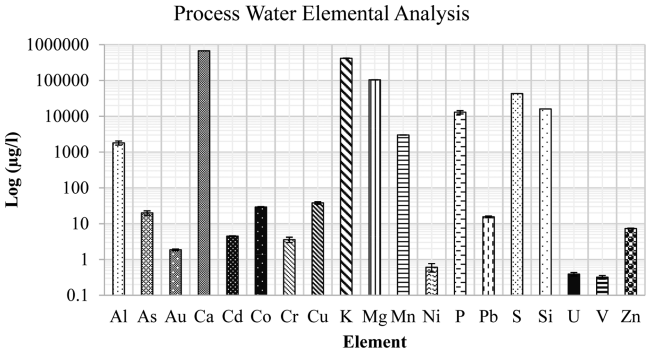

Figure 6. Major and trace elements in process water.

concentration of 1.86 μg/L is below the level considered economically viable for recovery from wastes (>2 g/ton).

2.7. Elemental Composition of Ash. Phytoremediation biomass from the acid mine drainage and polluted land can be expected to contain elevated concentrations of contaminants. In this case, the raw *S. lancea* biomass utilized for the hydrochar products was known to contain higher than average levels of sulfur and metals in tree biomass.[27] The concentrations of major and trace elements in the raw biomass, hydrochar, discard coal, and biocoal (hydrochar + discard coal) pellets at different weight percentages are depicted in Figures 7 and 8, respectively. The biocoal (BC) is a blend of

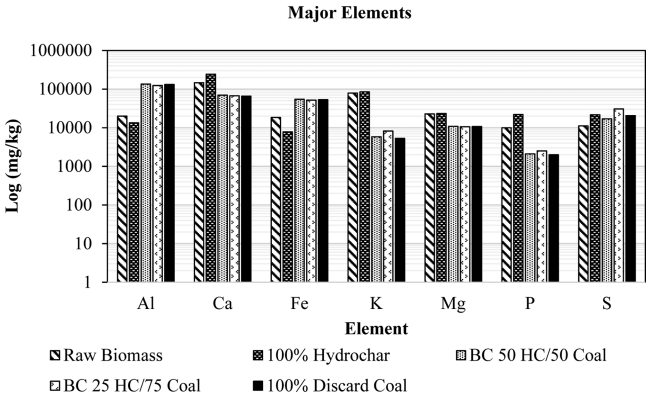

Figure 7. Concentrations of major components in the ash of raw biomass, hydrochar, coal, and hydrochar blends. $BC_{50\ HC/50\ C}$ denotes 50% hydrochar + 50% discard coal, and $BC_{25\ HC/75\ C}$: 25% hydrochar + 75% discard coal.

hydrochar and discard coal (C). Calcium is the most abundant element in all the samples analyzed in the raw biomass and hydrochar. The high concentration of Al obtained from the coal is expected, along with the increase as seen in the biocoal pellets made from the blends of discard coal and hydrochar. The concentration of Ca and P is higher in the ash content of the hydrochar, and this trend is similar to the result obtained by Poerschmann et al.[41] The concentrations of the plant macronutrients P, S, Ca, K, and Mg in the hydrochar are within the range for blending into fertilizer compounds. The concentrations of the plant micronutrients Fe, Cu, Co, Ni, Mn, and Zn are elevated, but are well within physiological norms for soil and blending in fertilizers. Mercury (Hg) was below detection limits, and the contaminants of concern As, Cd, Cr, Pb, and U were within regulatory guidelines and below plant toxicity levels, although V was in excess. Repeated application on land of such ash could lead to elevated

https://doi.org/10.1021/acsomega.1c02173
ACS Omega 2021, 6, 20292−20302

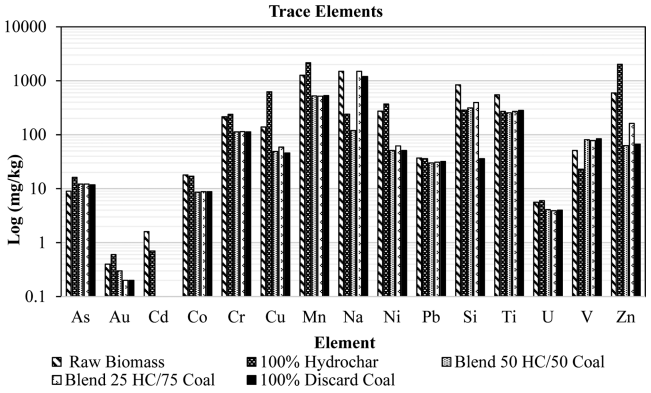

Figure 8. Concentrations of trace elements in the raw biomass, hydrochar, coal, and HTC hydrochar blends. $BC_{50\ HC/50\ C}$ denotes 50% hydrochar + 50% discard coal, and $BC_{25\ HC/75\ C}$: 25% hydrochar + 75% discard coal.

concentrations of potentially toxic elements in produce. Similar results were observed by Poerschmann et al.[41] for the dissolved organic matter phases from hydrothermal carbonization products.

The increase noted in some elements within the ash obtained from the hydrochar might be a result of the decomposition of minerals at high temperature during ashing. The blending of coal with this biomass has led to the reduction in most of the trace elements in the species and thereby provide an opportunity for its potential applications in other sectors. As a general guide to the suitability of the ash for different agronomic applications, the elemental concentrations of these ashes were compared to those of biomass fly ash as summarized by Fuller et al.[42] in a survey of the compliance limits for plant macro and micronutrients and non-nutrients in ash (Table 6). Most of the elements within the ash produced from the *S. lancea* biomass and coal utilized are within the European compliance maximum metal concentrations for fertilizers and applications to agricultural or forestry land. However, different limits may be relevant to the southern African soils, climate, and social setting when using ash from biomass produced on acid mine drainage.

Table 6. Compliance Concentrations for Metals in Biomass Fly Ash for Different Applications (Fuller et al.[42]) and the Range of HTC Ash Composition From This Study

Country	Finland	Finland	Germany	South Africa, acid mine drainage (this study)
use	forestry	agriculture	fertiliser	
		maximum metal content (mg/kg)		
As	30	25	40	9−16.2
Cd	17.5	1.5	1.5	0.1−1.6
Cu	700	600		46−625
Hg	1.0	1.0	1.0	0.1
Mn				518−2152
Ni	150	100	80	51−370
Pb	150	100	150	30−37
Zn	4500	1500		63−2011
Co				8.6−18
Cr	300	300		113−238

3. CONCLUSIONS

The hydrochar samples produced from species (*S. lancea*) planted for the consumption of polluted groundwater and for safe hydraulic control on the movement of groundwater plumes were assessed to establish their potential as a renewable fuel. In this study, the HTC process was used to produce new energy product "fuels" or alternative solid fuels, known as biocoal and biocoal/fine discard coal pellets. The study had shown that this solid fuel can be used as a substitute fuel for combustion in electricity generation due to its burning compatibility with the discard coal utilized. Future research will compare the concentration of gases released by the villagers while burning the traditional charcoal/coal and the pellets produced from this research, along with providing a detailed study on the re-use of the process water.

4. MATERIALS AND METHODS

4.1. Site Description. *S. lancea* were planted in 2003 and 2004 together with other tree species in site-species phytoremediation trials on polluted groundwater from gold and uranium tailings dam at AngloGold Ashanti Limited' West Wits and Vaal River mining operations in South Africa ("The Mine Woodlands Project").[22,23] The biomass for this study was harvested from trees grown on deep, red well-draining soils (South African Hutton form) over polluted groundwater from the Mispah gold and uranium tailings dam, Vaal River mining operations, near Orkney, South Africa. The tree growth, impact on groundwater and soil, and biomass production are reported elsewhere.[24−27,30] Four *S. lancea* trees were excavated and harvested at 12 years of age and divided into leaves, twigs, wood, dead wood, stump, root ball (coarse root), and roots (fine-medium root). The biomass was weighed, washed, and dried to ambient moisture content in a warehouse.

4.2. Sample Preparation. The different biomass components were milled in a Retsch SM 200 mill to <1 mm and <212 μm size fractions. After milling, the samples were tested for target size fractions by conducting a sieve analysis test and then placed in plastic bags. The <1 mm fraction was used for the hydrothermal carbonization and the <212 μm fraction for physicochemical characterization. The combination of tree materials from two trees (S11 and S12) for producing hydrochar and as cofired fuel with coal discard was based on the ash content of the compartments.

4.3. Analytical Methods and DTG Analysis. The proximate analysis was conducted following the ASTM D-5142, wherein around 1 g of sample was analyzed in a Leco TGA 701 instrument. The heat content was determined for the raw *S. lancea*, hydrochar, and the high ash discard coal using a Leco AC 500 calorimeter in accordance with ASTM D5865-04. The system uses an electronic thermometer with an accuracy of 0.0001 °C to measure the temperature every 6 s, with the results obtained within 4.5−7.5 min. The effect of hydrothermal treatment on the mass and energy yield of hydrochars was determined using the mass yield and energy yield equations as set out in eqs 4 and 5.[30] The mass yield η_M is obtained from the ratio of sample mass after HTC (M_t) and sample mass before HTC (M_o)

$$\eta_M = \left(\frac{M_t}{M_o}\right) \quad (4)$$

https://doi.org/10.1021/acsomega.1c02173
ACS Omega 2021, 6, 20292−20302

In calculating the energy yield, the gross calorific value for raw samples (GCV_u) and gross calorific value of the hydrochar (GCV_t) were used as shown in eq 2 below

$$\eta_E = \eta_M\left(\frac{GCV_t}{GCV_u}\right) \quad (5)$$

The reactivity test for all the samples (raw *S. lancea*, hydrochars, discard coal and different weight ratio of hydrochar/discard coal pellets) was conducted in a TGA under an air atmosphere at a heating rate of 6 °C/min, from 25 to 850 °C and held until there was a constant mass loss. An approximately 150 mg of fuel was used for each experiment. The combustion characteristics of the fuels tested are determined from the DTG curves generated from the individual fuel.

4.4. Experimental Design and Statistical Analysis. HTC process parameters were modeled using a response surface methodology (RSM) with CCD. CCD was used in this study to assess the impact of reaction temperature (T) and residence time (t) on the fuel characteristics. RSM/CCD is suitable for the optimization of process parameters and the analysis of the interaction between these parameters.[32−34] The structure and design matrix of the HTC experiments are shown in Table 7 with 11 experimental runs. There are four factorial points, four axial points, and three center points, which were repeated five times to obtain an accurate estimate of the experimental error and data reproducibility. Design-Expert software (version 11.1.2.0) from Stat-Ease, Inc. was used for the experimental design, model improvement, and analysis of variance (ANOVA).

Table 7. Experimental Design[a]

	factors_coded		factors_actual	
run order	T	T	T	t
1	0	0	240	60
2	1	−1	280	30
3	0	1	240	90
4	1	1	280	90
5	0	−1	240	30
6	−1	0	200	60
7	0	0	240	60
8	−1	−1	200	30
9	0	0	240	60
10	1	0	280	60
11	−1	1	200	90

[a]T—temperature in degrees Celsius; t—residence time in minutes.

4.5. Experimental Setup. The HTC experiments were conducted in a laboratory-scale high-pressure stirring Berghof BR-1500 reactor to produce different qualities of hydrochar. In each experiment, 100 g of air-dried biomass along with 800 mL of deionized water was fed into a stainless-steel vessel. The reactor contents were purged using argon gas at an initial pressure of 20 bar for each run, and the mixture agitated at 200 rpm until the end of the test. The reactor was heated to the required temperature and held for a certain time, as illustrated in Table 7. After the reaction, the reactor components were switched off and the reactor was left to cool naturally overnight. The reactor contents were separated using 609WS 240 mm filter paper discs into the liquid phase and the solid hydrochar. The solid hydrochar was subsequently oven-dried at 105 °C for 24 h, after which it was stored in plastic containers for further characterization tests. The hydrochar produced at 280 °C and residence time of 90 min was chosen as a superior product for hydrochar production and a blend for coal/hydrochar pellets. The mechanical properties of the discard coal/hydrochar pellets produced are described by Setsepu.[35]

4.6. Process Liquid Analysis. The process liquid from the hydrochar production during the hydrothermal process was analyzed for dissolved organic compounds using gas chromatography-mass spectrometry Shimadzu GCMS-2010. The oven temperature was initially set for 140 °C for 4 min and then increased to 250 °C at a heating rate of 4 °C/min with a holding time of 12.5 min, but the injection temperature was set at 220 °C using the split-less mode. The instrument was set according to the following parameters: sampling time: 1.00 min; flow control mode; pressure: 100.00 kPa, total flow: 50.00 mL/min; column flow: 1.13 mL/min; linear velocity: 3.00 mL/min. The identification of the organic compounds in the process liquid was conducted using the NIST 14 database and compared with published mass spectra.

4.7. Ashing and Ash Characterization. Five different samples were ashed and characterized for elemental composition. The raw biomass sample and 100% hydrochar were ashed according to the CEN/TS 14,588 standard method for ashing biomass. The blended samples with 50% coal discard or more were ashed in accordance with ISO 1171:2010 for coal ashing. Microwave-assisted digestion of 0.5 g ash in 9 mL nitric acid (HNO_3) and 3 mL hydrochloric acid (HCl) was then conducted on the five samples. The major elements in the ash dissolution were determined using (ICP−AES), and trace elements were determined using a PerkinElmer NexION 300X ICP−MS (KED mode). The same methods were used for the elemental analyses of the major and trace elements in the process water obtained from the pressurized hydrothermal vessel. The calibration standard ranged from 0 (blank) to 10 μg/L, with scandium (Sc) and iridium (Ir) added to all samples as internal standards, and NIST 1640 used to verify the calibration curves.

AUTHOR INFORMATION

Corresponding Author

Samson O. Bada − *DSI/NRF Clean Coal Technology Research Group, School of Chemical and Metallurgy, Faculty of Engineering and the Built Environment, University of the Witwatersrand, Johannesburg 2050, South Africa;* orcid.org/0000-0002-1079-3492; Email: Samson.Bada@wits.ac.za

Authors

Ramadimetja L. Setsepu − *DSI/NRF Clean Coal Technology Research Group, School of Chemical and Metallurgy, Faculty of Engineering and the Built Environment, University of the Witwatersrand, Johannesburg 2050, South Africa*

Jibril Abdulsalam − *DSI/NRF Clean Coal Technology Research Group, School of Chemical and Metallurgy, Faculty of Engineering and the Built Environment, University of the Witwatersrand, Johannesburg 2050, South Africa;* orcid.org/0000-0001-5072-4996

Isabel M. Weiersbye − *Ecological Engineering and Phytotechnology Programme (EEPP), School of Animal, Plant and Environmental Sciences, University of the Witwatersrand, Johannesburg 2050, South Africa*

https://doi.org/10.1021/acsomega.1c02173
ACS Omega 2021, 6, 20292−20302

Complete contact information is available at:
https://pubs.acs.org/10.1021/acsomega.1c02173

Notes

The authors declare no competing financial interest.

■ ACKNOWLEDGMENTS

This study forms part of the first author's M.Sc. dissertation, and her research was supported by the National Research Foundation (NRF) of South Africa's SARChI Clean Coal Technology Grant 86421 to S.O.B. and by the Eskom Tertiary Education Support Program, 2018. The Mine Woodlands Project was funded by AngloGold Ashanti Ltd South Africa Environmental Management Department and the Department of Trade and Industry of South Africa THRIP to I.M.W. and E. T. F. Witkowski. Opinions, findings, and conclusions expressed are those of the authors.

■ REFERENCES

(1) Kambo, H. S.; Dutta, A. A comparative review of biochar and hydrochar in terms of production, physico-chemical properties, and applications. *Renewable Sustainable Energy Rev.* **2015**, *45*, 359−378.
(2) Smith, A. M.; Whittaker, C.; Shield, I.; Ross, A. B. The potential for production of high quality bio-coal from early harvested Miscanthus by hydrothermal carbonisation. *Fuel* **2018**, *220*, 546−557.
(3) Hoekman, S. K.; Broch, A.; Felix, L.; Farthing, W. Hydrothermal carbonization (HTC) of loblolly pine using a continuous, reactive twin-screw extruder. *Energy Convers. Manage.* **2017**, *134*, 247−259.
(4) Wang, T.; Zhai, Y.; Zhu, Y.; Li, C.; Zeng, G. A review of the hydrothermal carbonization of biomass waste for hydrochar formation: process conditions, fundamentals, and physicochemical properties. *Renewable Sustainable Energy Rev.* **2018**, *90*, 223−247.
(5) Reza, M. T.; Uddin, M. H.; Lynam, J. G.; Hoekman, S. K.; Coronella, C. J. Hydrothermal carbonization of loblolly pine: Reaction chemistry and water balance. *Biomass Convers. Biorefin.* **2014**, *4*, 311−321.
(6) Danso-Boateng, E.; Shama, G.; Wheatley, A. D.; Martin, S. J.; Holdich, R. G. Hydrothermal carbonisation of sewage sludge: Effect of process conditions on product characteristics and methane production. *Bioresour. Technol.* **2015**, *177*, 318−327.
(7) Libra, J. A.; Ro, K. S.; Kammann, C.; Funke, A.; Berge, N. D.; Neubauer, Y.; Titirici, M.-M.; Fühner, C.; Bens, O.; Kern, J.; Emmerich, K.-H. Hydrothermal carbonization of biomass residuals: A comparative review of the chemistry, processes and applications of wet and dry pyrolysis. *Biofuels* **2011**, *2*, 71−106.
(8) Park, K. Y.; Lee, K.; Kim, D. Characterized Hydrochar of Algal Biomass for Producing Solid Fuel through Hydrothermal Carbonization. *Bioresour. Technol.* **2018**, *258*, 119−124.
(9) Yeoh, K.-H.; Shafie, S. A.; Al-Attab, K. A.; Zainal, Z. A. Upgrading agricultural wastes using three different carbonization methods: thermal, hydrothermal and vapothermal. *Bioresour. Technol.* **2018**, *265*, 365−371.
(10) Saba, A.; Saha, P.; Reza, M. T. Co-hydrothermal carbonization of coal-biomass blend: influence of temperature on solid fuel properties. *Fuel Process. Technol.* **2017**, *167*, 711−720.
(11) Lu, L.; Namioka, T.; Yoshikawa, K. Effects of hydrothermal treatment on characteristics and combustion behaviours of municipal solid wastes. *Appl. Energy* **2011**, *88*, 3659−3664.
(12) Prawisudha, P.; Namioka, T.; Yoshikawa, K. Coal alternative fuel production from municipal solid wastes employing hydrothermal treatment. *Appl. Energy* **2012**, *90*, 298−304.
(13) Lin, Y.; Ma, X.; Peng, X.; Yu, Z. Hydrothermal carbonization of typical components of municipal solid waste for deriving hydrochars and their combustion behavior. *Bioresour. Technol.* **2017**, *243*, 539−547.
(14) Ismail, T. M.; Yoshikawa, K.; Sherif, H.; Abd El-Salam, M. Hydrothermal treatment of municipal solid waste into coal in a commercial Plant: Numerical assessment of process parameters. *Appl. Energy* **2019**, *250*, 653−664.
(15) Lee, J.; Sohn, D.; Lee, K.; Park, K. Y. Solid fuel production through hydrothermal carbonization of sewage sludge and microalgae Chlorella sp. From wastewater treatment plant. *Chemosphere* **2019**, *230*, 157−163.
(16) Cao, X.; Ro, K. S.; Chappell, M.; Li, Y.; Mao, J. Chemical Structures of Swine-Manure Chars Produced under Different Carbonization Conditions Investigated by Advanced Solid-State 13C Nuclear Magnetic Resonance (NMR) Spectroscopy. *Energy Fuels* **2011**, *25*, 388−397.
(17) Silakova, M. Hydrothermal Carbonization of the tropical biomass. M.Sc. Dissertation, Lappeenranta University of Technology, Finland, 2018, p 60.
(18) Zhu, Y.; Si, Y.; Wang, X.; Zhang, W.; Shao, J.; Yang, H.; Chen, H. Characterization of hydrochar pellets from hydrothermal carbonization of agricultural residues. *Energy Fuels* **2018**, *32*, 11538−11546.
(19) Hoekman, S. K.; Broch, A.; Warren, A.; Felix, L.; Irvin, J. Laboratory pelletization of hydrochar from woody biomass. *Biofuels* **2014**, *5*, 651−666.
(20) Lu, X.; Jiang, J.; He, J.; Sun, K.; Sun, Y. Synergy of Hydrothermal and Organic Acid Washing Treatments in Chinese Fir Wood Vinegar Preparation. *ACS Omega* **2020**, *5*, 13685−13693.
(21) Weiersbye, I. M.; Witkowski, E. T. F.; Reichardt, M. Floristic composition of gold and uranium tailings dams, and adjacent polluted areas, on South Africa's deep-level mines. *Bothalia* **2006**, *36*, 101−127.
(22) Weiersbye, I. M. Global review and cost comparison of conventional and phytotechnologies for mine closure. In *Mine Closure 2007 Proceedings of the 2nd International Seminar on Mine Closure*; Fourie, A. B., Tibbett, M., Wiertz, J., Eds.; Santiago, 2007. 978-0-9804185-0-7, pp 13−19.
(23) Dye, P. J.; Weiersbye, I. M. The Mine Woodlands Project in the Witwatersrand Basin gold fields of South Africa: strategy and progress. *Proceedings of the International Mine Water Association*; Wolkersdorfer, I., Eds.; IMWA 2010: Novia Scotia, Canada, 2010, pp 471−474.
(24) Dye, P. J.; Jarmain, C.; Oageng, B.; Xaba, J.; Weiersbye, I. M. The potential of woodlands and reed-beds for control of acid mine drainage in the Witwatersrand gold fields, South Africa. *Proceedings of the 3rd International Conference on Mine Closure*; Fourie, A. B., Tibbett, M., Weiersbye, I. M., Eds.; Australian Centre for Geomechanics, University of Western Australia: Sandton, South Africa, 2008, pp 487−497.
(25) Dye, P.; Naiken, V.; Clulow, A.; Prinsloo, E.; Crichton, M.; Weiersbye, I. Sap flow in Searsia pendulina and Searsia lancea trees established on mining sites in central South Africa. *S. Afr. J. Bot.* **2017**, *109*, 81−89.
(26) Grindley, S. Modelling the effects of trees on a contaminated groundwater plume from a gold tailings storage facility in the Orkney district. M.Sc. Thesis, The University of the Witwatersrand, Johannesburg, South Africa, 2014.
(27) Joubert, M. Contaminant fate in Searsia lancea woodlands on acid mine drainage in the Witwatersrand Basin gold fields. M.Sc. Dissertation, University of the Witwatersrand, 2018, p 123.
(28) Mosito, N. S. V. Risk assessment of above ground biomass for fuel use in Eucalptus species cultivated on acid mine drainage in the Witwatersrand Basin gold fields. MSc Dissertation, University of the Witwatersrand, Johannesburg, 2016.
(29) Ndou, N. R.; Bada, S. O.; Falcon, R. M. S.; Weiersbye, I. M. Co-combustion of Searsia lancea and Tamarix usneoides with high ash coal. *Fuel* **2020**, *267*, 117282.
(30) Mokgalaka-Matlala, N. S.; Combrinck, S.; Regnier, T.; Weiersbye, I. M.; Kouekam, C.; Lepule, P. Selection of tree species as assets for mine phytoremediation using the genus Searsia (Anacardiaceae) as a model. In *Mine Closure 2010: proceedings of the 5th International Conference on Mine Closure November 2010*; Fourie, A. B., Tibbett, M., Wiertz, J., Eds.; Australian Centre for Geomechanics, University of Western Australia: Santiago, Chile, 2010.

(31) Makwarela, M. O.; Bada, S. O.; Falcon, R. M. S. Co-firing combustion characteristics of different ages of Bambusa balcooa relative to a high ash coal. *Renewable Energy* **2017**, *105*, 656−664.
(32) Sureshkumar, A.; Susmita, M. Optimization of preparation conditions for activated carbons from polyethylene terephthalate using response surface methodology. *Braz. J. Chem. Eng.* **2018**, *35*, 1105−1116.
(33) Xin-hui, D.; Srinivasakannan, C.; Jin-sheng, L. Process optimization of thermal regeneration of spent coal based activated carbon using steam and application to methylene blue dye adsorption. *J. Taiwan Inst. Chem. Eng.* **2014**, *45*, 1618−1627.
(34) Zhao, W.; Fierro, V.; Zlotea, C.; Aylon, E.; Izquierdo, M. T.; Latroche, M.; Celzard, A. Optimization of activated carbons for hydrogen storage. *Int. J. Hydrogen Energy* **2011**, *36*, 11746−11751.
(35) Setsepu, R. L. The utilisation of Searsia lancea and Tamarix usneoides as feedstock for biochar production through hydrothermal carbonisation. M.Sc. Dissertation, University of the Witwatersrand, Johannesburg, South Africa, 2020, p 126.
(36) Fakkaew, K.; Koottatep, T.; Pussayanavin, T.; Polprasert, C. Hydrochar production by hydrothermal carbonization of faecal sludge. *J. Water, Sanit. Hyg. Dev.* **2015**, *5*, 439−447.
(37) Hoekman, S. K.; Broch, A.; Robbins, C.; Zielinska, B.; Felix, L. Hydrothermal carbonization (HTC) of selected woody and herbaceous biomass feedstocks. *Biomass Convers. Biorefin.* **2013**, *3*, 113−126.
(38) Sahu, J. N.; Acharya, J.; Meikap, B. C. Optimization of production conditions for activated carbons from Tamarind wood by zinc chloride using response surface methodology. *Bioresour. Technol.* **2010**, *101*, 1974−1982.
(39) Bezener, M. A. Bayesian spatiotemporal modelling using hierarchical spatial priors with applications to functional magnetic resonance imaging. Ph.D. Thesis, University of Minnesota, Minnesota, USA, 2015XXX pages.
(40) Köchermann, J.; Görsch, K.; Wirth, B.; Mühlenberg, J.; Klemm, M. Hydrothermal carbonization: temperature influence on hydrochar and aqueous phase composition during process water recirculation. *J. Environ. Chem. Eng.* **2018**, *6*, 5481−5487.
(41) Poerschmann, J.; Weiner, B.; Wedwitschka, H.; Baskyr, I.; Koehler, R.; Kopinke, F.-D. Characterization of Biocoals and Dissolved Organic Matter Phases Obtained upon Hydrothermal Carbonization of Brewer's Spent Grain. *Bioresour. Technol.* **2014**, *164*, 162−169.
(42) Fuller, A.; Carbo, M.; Savat, P.; Kalivodova, J.; Maier, J.; Scheffknecht, G. Results of fly ash quality for disposal options from high thermal shares up to pure biomass combustion in a pilot-scale and large-scale pulverized fuel power plants. *Renewable Energy* **2015**, *75*, 899−910.

https://doi.org/10.1021/acsomega.1c02173
ACS Omega 2021, 6, 20292−20302